# Analysis of the dynamic behavior of a truss bridge

## MECA-0029 - Theory of Vibration


**Group** 40

**Casimir Fayt**


Professor
Pr. Jean-Claude Golinval

Assistant
Ir. Laura Prijot

Academic year
2019 - 2020

# Contents

# Introduction

The work made throughout this report rests on the *Finite Element Method*, in the field of the *Vibration Theory*. This theory has been introduced at the end of the $XIX^{th}$ century by Lord Rayleigh, and is nowadays based on the *variational approach*. The principle of oscillation about an equilibrium configuration represented an unsuspected source of predictable knowledge, mainly over today structures as planes, buildings, bridges, etc.

But such structural analysis was time-costly and very complicated to achieve. One had to wait for the advent of the computer age, which arrived in the second half of the $XX^{th}$ century. Computational power, thanks to discretisation and use of matrices, allowed to tackle ever-growing problem size.

## Structure studied

The structure under study here is a truss bridge of twenty meters length, for meters wide and three meters high in steel. The system is in three dimensions, and evaluated for six degrees of freedom, corresponding to the three translational and the three rotational degrees of freedom. The structure has boundary conditions : the four extreme nodes in the $z = 0$ plane are constrained. The nodes for $y_{max} = 20$ m are clamped, which means that they don't have any translational degree of freedom. The nodes for $y_{min} = 0$ m are supported, which corresponds to only the translational $z$-oriented degree of freedom blocked.

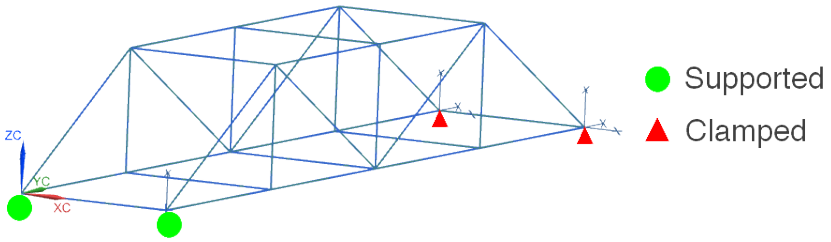


Figure 1: Truss structure as modelised in Siemens NX 12.0

The truss bridge is simplified for modelisation by simulating the beams as lines. All beams are made in the same material : steel. Their main mechanical properties are

$$\rho = 7\,800 \text{ kg.m}^{-3} \qquad E = 210 \text{ GPa} \qquad \nu = .3 \tag{0.1}$$

The beams have two different sections. The eight diagonal ones have a rectangular cross section of thirty millimetres wide and eighty millimetres high. Their orientation is such that the height lies in the vertical plane. All the other beams have a square cross section of seventy millimetres edges.

## Organisation of the report

The first section of this report will present the modelisation of the structure. This first step is paramount as it is compulsory to any FEM method. A model will be built using MatLab, and another one will be modelised thanks to Siemens NX, using the Samcef solver. The latter one will account for exact calculations, and will be used to compare accuracy of the MatLab model results.

The following section is dedicated to extracting eigenfrequencies of the structure thanks to structural analysis, and to the study of the *modal behaviour* of the model. The model will be enhanced by introducing a damping in the model. This damping is introduced thanks to the *proportional damping assumption*, which will allow to compute easily the damping ratios for each eigenfrequency. The damping will be computed such that the two first damping ratios are equal to $1\%$.

The third section will go further into simulation by studying the *forced harmonic response*. This is achieved by introducing a dynamic load at a node, and by computing the response displacements at another node as would measure a three-dimensional accelerometer. Such vectors are calculated through two family of methods : the *modal superposition* and the *direct time integration*.

For the first family, the modal displacement and the modal acceleration methods are implemented. The first one uses a truncature of weighted eigenmodes superposition. The second one follow the same idea, with a corrective term depending on the dynamic load.

For the second family, the *Newmark* integration scheme is used. This method is based on an iterative predictive corrective routine, using a iterative matrix linked to the equilibrium equation of the system

The next step studies the *reduction methods*, allowing to condense the model and save computation time. Such methods efficiency are given by their accuracy on the eigenfrequencies compared to the computation time decrease. Two methods are implemented : the static *Guyan-Irons method* and the dynamic *Craig-Bampton method*. Efficiency are compared, and both are further analysed thanks to the direct time integration scheme.

The final step of the report will recall main ideas of the work, how the studies were performed as well as the main results.

# 1 Modal behaviour

## 1.1 Discretisation

The first step of the *Finite Element Method* is to divide the structure into kinematically admissible elements. The easiest way is obviously by selecting each beam as an element. The structure then presents $34$ beams and $16$ nodes. To enhance calculations, one may discretise the beams into elements. To do so, each beam is discretised into a certain number of elements, giving the level of discretisation. For example, the structure discretised in five elements per beam is represented in figure 2.

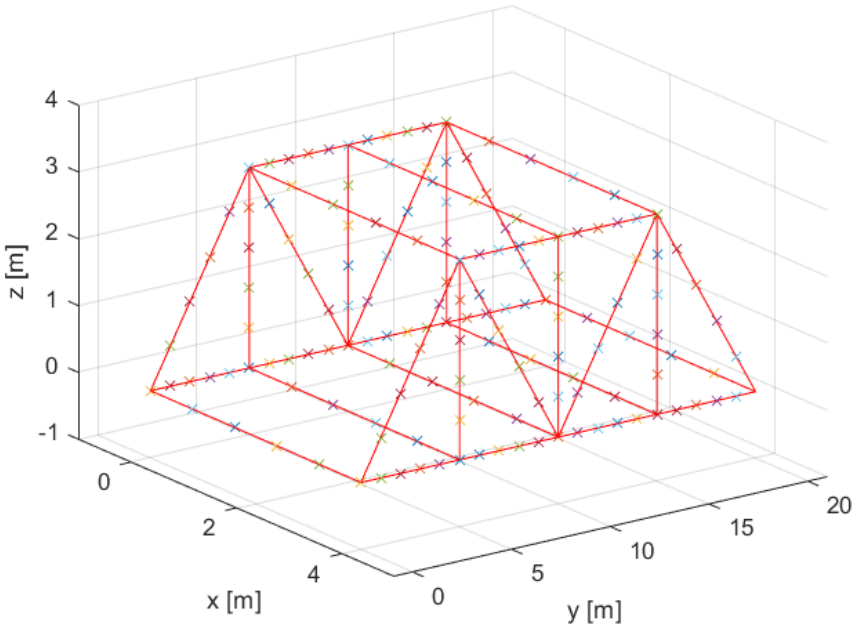


Figure 2: Discretisation of the structure in 5 elements

## 1.2 Eigenfrequencies

Thanks to discretisation and *FEM*, the natural frequencies may be computed and the corresponding mode shapes simulated. The accuracy of such calculations depends on the discretisation level and increases the computation time. The *proportional damping assumption* finally allows to compute a light damping in the model, accounting for a damping ratio equal to $1\%$ for the two first modes.

### 1.2.1 Computation

To extract the natural frequencies of oscillation of the truss bridge. Through the variational approach, a law is established linking kinematic and potential energies $T_e$ and $V_e$. Both terms are linked to each element (according to the element's properties), and to the element degrees of

freedom (linked to its initial and final node). The six degrees of freedom of each node are given by the local translations $(u, v, w)$ and rotations $(\psi_x, \psi_y, \psi_z)$ :

$$\boldsymbol{q}_e^T = [u_1 \quad v_1 \quad w_1 \quad \psi_{x1} \quad \psi_{y1} \quad \psi_{z1} \quad u_2 \quad v_2 \quad w_2 \quad \psi_{x2} \quad \psi_{y2} \quad \psi_{z2}] \tag{1.1}$$

Thanks to the vector of local displacement of the element, the kinematic and potential energies are given by

$$T_e = \frac{1}{2}\, \dot{\boldsymbol{q}}_e^T\, M_e\, \dot{\boldsymbol{q}}_e \qquad\qquad V_e = \frac{1}{2}\, \boldsymbol{q}_e^T\, K_e\, \boldsymbol{q}_e \tag{1.2}$$

Where

- $\boldsymbol{q}_e$ is the vector of structural displacement, for each degree of freedom
- $K_e$ is the elementary stiffness matrix
- $M_e$ is the elementary mass matrix

Both elementary matrices represents the interaction of the shape functions yielding the spatial dependence of displacement of the degrees of freedom movement as

$$u(x,t) = \boldsymbol{\Phi}_e(x,y,z)\; \boldsymbol{q}_e(t) \tag{1.3}$$

They are given for a 3D problem with 6 degrees of freedom in the statement. Such matrices are assembled for each element, taking into account its mechanical properties (moment of inertia, Young's modulus, shear modulus, etc) and geometric properties (cross section, initial and final node, orientation, boundary conditions, etc). They are expressed in the structural axis thanks to the rotation matrix $\boldsymbol{R}_e$ linking the local axis $0xyz$ to the structural axis $0XYZ$ :

$$\boldsymbol{T}_e = \begin{bmatrix} \boldsymbol{R}_e & 0 & 0 & 0 \\ 0 & \boldsymbol{R}_e & 0 & 0 \\ 0 & 0 & \boldsymbol{R}_e & 0 \\ 0 & 0 & 0 & \boldsymbol{R}_e \end{bmatrix} \text{ with } \boldsymbol{R}_e = \begin{bmatrix} \boldsymbol{e}_X \cdot \boldsymbol{e}_x & \boldsymbol{e}_Y \cdot \boldsymbol{e}_x & \boldsymbol{e}_Z \cdot \boldsymbol{e}_x \\ \boldsymbol{e}_X \cdot \boldsymbol{e}_y & \boldsymbol{e}_Y \cdot \boldsymbol{e}_y & \boldsymbol{e}_Z \cdot \boldsymbol{e}_y \\ \boldsymbol{e}_X \cdot \boldsymbol{e}_z & \boldsymbol{e}_Y \cdot \boldsymbol{e}_z & \boldsymbol{e}_Z \cdot \boldsymbol{e}_z \end{bmatrix} \tag{1.4}$$

This yields the elementary matrices in the structural axis as

$$\boldsymbol{K}_{eS} = \boldsymbol{T}_e^T \boldsymbol{K}_{eL} \boldsymbol{T}_e^T \qquad \boldsymbol{M}_{eS} = \boldsymbol{T}_e^T \boldsymbol{M}_{eL} \boldsymbol{T}_e^T \tag{1.5}$$

The structural matrices are finally obtained by taking into account the elementary matrices expressed in the structural axis of all elements, using the localisation matrix which allows to select the structural degrees of freedom corresponding to the degrees of freedom of the element under study. Those structural matrices are used for the eigenvalue problem :

$$\boldsymbol{K}\, \boldsymbol{q} = \omega^2\, \boldsymbol{M}\, \boldsymbol{q} \tag{1.6}$$

### 1.2.2 Convergence

Increasing the discretisation level of the problem enhances precision as more and more degrees of freedom will be taken into account, allowing for better evaluation of the natural frequencies. The discretisation of the structure is made by splitting each beam into elements of equal length. Each element inherits the mechanical and geometrical properties of its mother beam (apart from the length). Nonetheless, such deeper discretisation grows the problem size, making the resolution of the eigenvalue problem longer to compute. A trade-off must be chosen. A study of convergence and time of computation has been performed on the program, the data resulting are presented in table 1.1.

To account for the exact natural frequencies, the structure has been modelised in Siemens NX 12.0. The fifty first eigenmodes have been computed and compared with the fifty first eigenmodes of the script written using the finite element method. The relative error between each natural frequency for each discretisation level and the exact one given by NX has been computed, and an arithmetical average has been calculated to compare convergence according to discretisation level.

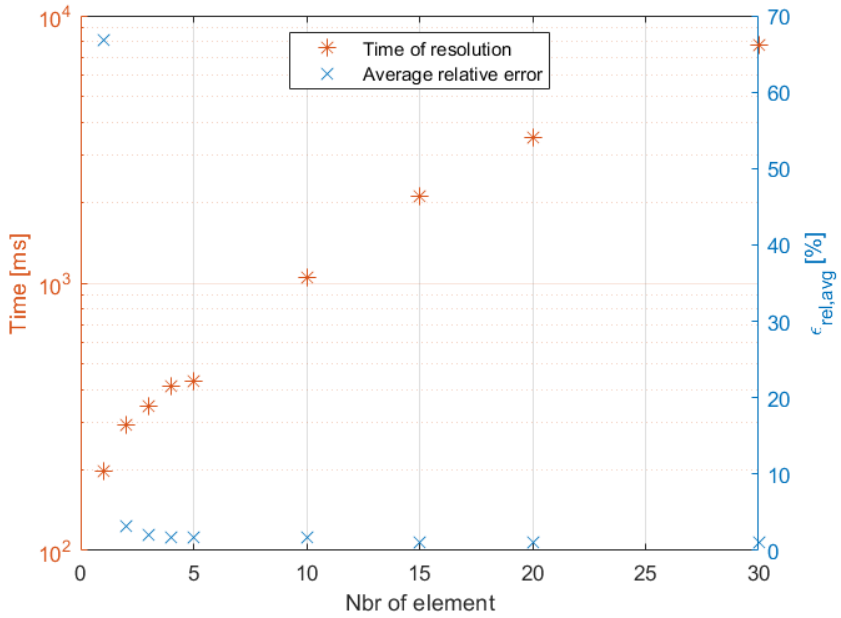


Figure 3: Convergence of relative error and computation time for different discretisation levels
Data available in table 1.1

| Nbr of elements | $\varepsilon_{rel,avg}$ | Time of discretisation [ms] | Time of resolution [ms] | Problem size |
|---|---|---|---|---|
| 1 | 66.84% | 24.289 | 197.258 | $88 \times 88$ |
| 2 | 3.18% | 42.597 | 294.693 | $292 \times 292$ |
| 3 | 2.01% | 53.757 | 346.871 | $496 \times 496$ |
| 4 | 1.78% | 63.702 | 413.507 | $700 \times 700$ |
| 5 | 1.70% | 54.511 | 428.490 | $904 \times 904$ |
| 10 | 1.64% | 73.359 | 1050.147 | $1924 \times 1924$ |
| 15 | 1.02% | 78.455 | 2101.075 | $2944 \times 2944$ |
| 20 | 1.02% | 97.113 | 3508.331 | $3964 \times 3964$ |
| 30 | 1.02% | 119.379 | 7790.724 | $6004 \times 6004$ |

Table 1.1: Convergence of discretisation

The analysis of the data shown in tab 1.1 shows that on the one hand the discretisation time stays negligible : from 24 ms up to 120 ms roughly. On the other hand, the time needed to solve the eigenvalue problem increases exponentially. The evolution according to the discretisation level in figure 3 is plotted on a logarithmic scale. Nonetheless, the relative error is less than $5\%$ as soon as the number of elements reaches two. The relative error reaches an asymptotic value of $1.02\%$. This discrepancy between SIEMENS and MATLAB may be explained by some differences between the properties taken into account between the two solvers. Indeed, SIEMENS takes into account other values for beam deformations (shear, torsion, etc).

Eventually, one may conclude to this analysis that a discretisation of each beam into five elements is the best trade-off for accuracy on the natural frequencies and small computation time. Choosing $N_{elem} = 5$, the eight first natural frequencies of the structure, computed by the finite element method, are given in table 1.2 page 8.

### 1.2.3 Mode shapes

The mode shapes of the structure may be drawn, to represent graphically the deformation of the beams. They are extracted from the resulting matrix of the eigenvalue problem 1.6. It has to be noted that the computation times are different than the ones shown in table 1.1, because further than calculating the eigenvalues of the system, the program needs now to calculate the resulting matrix with eigenvectors. The three first modes have been simulated on MATLAB (with an average computation time of 3791.342 ms) and on SIEMENS NX. As shown in the figure 4, the mode shapes computed are the same.

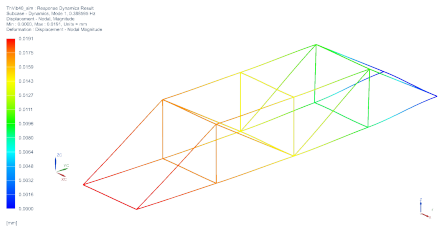

(a) Siemens NX
$f = 0.389$ Hz

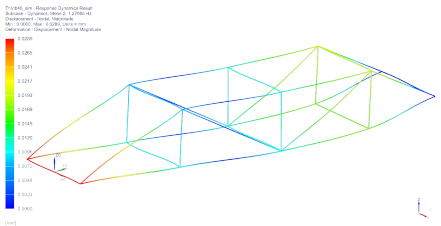

(c) Siemens NX
$f = 1.271$ Hz

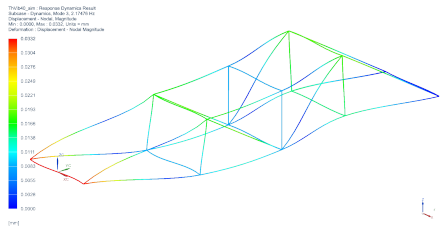

(e) Siemens NX
$f = 2.176$ Hz

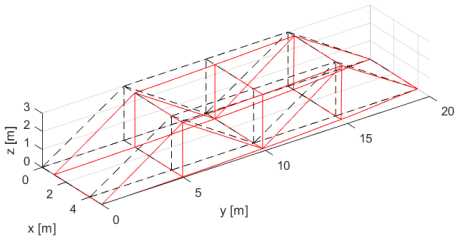


(b) Matlab
$f = 0.393$ Hz

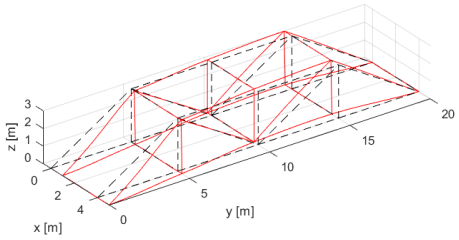


(d) Matlab
$f = 1.286$ Hz

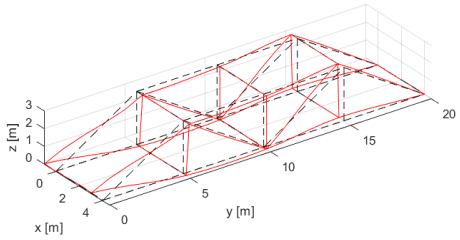


(f) Matlab
$f = 2.198$ Hz

Figure 4: Three first natural mode shapes of the structure

### 1.2.4 Damping

The current model with the elementary stiffness and mass matrices does not account for damping in the structure. A damping matrix will be constructed, following the *proportional assumption*. This allows for considering a light damping of the structure. The damping matrix is then assumed mainly weighted on its diagonal, allowing to construct it as

$$\boldsymbol{C} = a\boldsymbol{K} + b\boldsymbol{M} \tag{1.7}$$

Which yields a damping ratio expressed as

$$\varepsilon_r = \frac{1}{2}\left(a\omega_{0r} + \frac{b}{\omega_{0r}}\right) \tag{1.8}$$

Knowing that a damping ratio of $1\%$ is asked for the two first eigenmodes, the previous equations yield a solvable system with two unknowns : the parameters $a$ and $b$.

$$\begin{bmatrix} .5\omega_1 & \frac{.5}{\omega_1} \\ .5\omega_2 & \frac{.5}{\omega_2} \end{bmatrix} \begin{bmatrix} a \\ b \end{bmatrix} = \begin{bmatrix} .01 \\ .01 \end{bmatrix} \tag{1.9}$$

Which gives as result :

$$a = 1.896553\ 10^{-3}\ \text{s} \qquad b = 3.779232\ 10^{-2}\ \text{Hz} \tag{1.10}$$

The Rayleigh damping matrix $\boldsymbol{C}$ may eventually be calculated by 1.7 using the coefficients from 1.10. The damping ratios and natural frequencies for the eight first modes read :

| Mode number | $\omega$ [rad.Hz] | $f$ [Hz] | $\varepsilon$ [%] |
|---|---|---|---|
| 1 | 2.467 | 0.393 | 1.00 |
| 2 | 8.079 | 1.286 | 1.00 |
| 3 | 13.812 | 2.198 | 1.45 |
| 4 | 20.446 | 3.254 | 2.03 |
| 5 | 23.978 | 3.816 | 2.35 |
| 6 | 26.030 | 4.143 | 2.54 |
| 7 | 27.212 | 4.331 | 2.65 |
| 8 | 27.457 | 4.370 | 2.67 |

Table 1.2: The eight first natural frequencies and damping ratios of the structure
Computed with $N_{elem} = 5$

# 2 Dynamic response

As the previous section studied the modelisation of the truss structure without any exterior intervention, it would be now interesting to take a look at the response of the structure to an harmonic excitation. The equation of motion for the free model was governed by the equation

$$\boldsymbol{M}\ddot{\boldsymbol{q}} + \boldsymbol{C}\dot{\boldsymbol{q}} + \boldsymbol{K}\boldsymbol{q} = 0 \tag{2.1}$$

To study the harmonic response of the structure, an external load is considered. This load adds in the previous equation by modifying the right-hand side :

$$\boldsymbol{M}\ddot{\boldsymbol{q}} + \boldsymbol{C}\dot{\boldsymbol{q}} + \boldsymbol{K}\boldsymbol{q} = \boldsymbol{p}(t) \tag{2.2}$$

In this case, the load is represented by a chirped sinus signal of maximal amplitude of $250$ N. The initial frequency is $f_0 = 0$Hz, while the maximum frequency of $f = 10$ Hz is reached at the time $t = 40$s. Such external load allows to excite all frequencies between zero and ten hertz. This range contains all the eight first natural frequencies of the structure. This external load is applied at the node $(4, 5, 0)$ in the direction parallel to the width of the bridge, which corresponds to the structural $X$ axis.

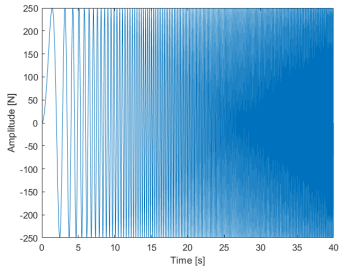


Figure 5: Applied load : sinusoidal chirped signal

The harmonic response of the structure may be computed according to two main families of methods : the **modal superposition methods** and the **direct time integration**.

The modal superposition method rests on the modal expansion of the harmonic response, which correspond in a sum expansion of weighted mode shapes. Under the assumption that the solution lies in a subspace of the eigenmodes basis, the sum is truncated to avoid large computation times, at the cost of accuracy.

The modal acceleration method adds a corrective term to the modal expansion of the modal displacement method.

The direct time integration consists in a numerical integration in an iterative routine of prediction and correction. The numerical integration is greatly sensitive to the time step chosen.

## 2.1 Modal displacement method

The modal displacement method consists in expressing the response vector through a modal expansion in a basis formed by the eigenmodes. The total expression then takes the following expression

$$\boldsymbol{q}(t) = \sum_{r=1}^{n} \eta_r(t) \boldsymbol{x}_r \tag{2.3}$$

Where $n$ is the number of modes, and $\eta_r(t)$ are the normal coordinates. The normal coordinates are solutions of the $n$ uncoupled normal equations which take into account the external load :

$$\begin{aligned} \ddot{\eta}_r + 2\varepsilon_r \omega_r \dot{\eta}_r + \omega_r^2 \eta_r &= \phi_r(t) \\ \phi_r(t) &= \frac{\boldsymbol{x}_r^T \boldsymbol{p}(t)}{\mu_r} \end{aligned} \tag{2.4}$$

Such equation is a second degree differential equation. Its solution is given by

$$\eta_r(t) = e^{-\varepsilon_r \omega_r t} \left[ A \cos\left(\omega_r^{(d)} t\right) + B \sin\left(\omega_r^{(d)} t\right) \right] + \int_0^t \phi_r(\tau) h_r(t-\tau) d\tau \tag{2.5}$$

from this expression are extracted the initial conditions on displacement and velocity, as by (2.3) we have that $\boldsymbol{q}(0)$ and $\dot{bmq}$ are directly linked to $\eta_r(0)$ and $\dot{\eta}_r$ :

$$\begin{aligned} \boldsymbol{q}(0) &= \eta_r(0) = A \\ \dot{\boldsymbol{q}}(0) &= \dot{\eta}_r(0) = -B \end{aligned} \tag{2.6}$$

The easiest way is taking null initial conditions, leading to $A = B = 0$. The initial condition for the acceleration is then directly given by the equation of motion, yielding

$$\ddot{\boldsymbol{q}}(0) = \boldsymbol{M}^{-1} \boldsymbol{p}(0) \tag{2.7}$$

In (2.5) the impulse response is given by

$$h_r(t) = \begin{cases} \dfrac{e^{-\varepsilon_r \omega_r t} \sin\left(\omega_r^{(d)} t\right)}{\omega_r^{(d)}} & t > 0 \\ 0 & t \leq 0 \end{cases} \tag{2.8}$$

And the damped natural angular frequencies are given by

$$\omega_r^{(d)} = \omega_r \sqrt{1 - \varepsilon_r^2} \tag{2.9}$$

Now, all terms in 2.5 are known and the normal coordinates may be calculated for each mode. However, the principle beneath the modal displacement method is to truncate the serie (2.3) in a subspace of the basis, retaining only a certain number of nodes $k < n$ :

$$\boldsymbol{q}(t) = \sum_{r=1}^{k} \eta_r(t) \boldsymbol{x}_r \tag{2.10}$$

The accuracy of the results will depend on the number of modes retained $k$ and on the time step $h$.

A useful value is the M-norm of the response vector, computed as

$$\|\boldsymbol{q}\|_M^2 = \boldsymbol{q}^T \, \boldsymbol{M} \, \boldsymbol{q} \tag{2.11}$$

This expression, with spectral expansions of the terms, finally leads to

$$\|\boldsymbol{q}\|_M^2 = \underbrace{\sum_{s=1}^{k} \frac{(\boldsymbol{x}_{(s)}^T \boldsymbol{g})^2}{\mu_s}}_{\text{spatial factor}} * \underbrace{\left( \frac{1}{\omega_s} \int_0^t \sin\left(\omega_s (t-\tau)\right) \phi(\tau) d\tau \right)^2}_{\text{temporal factor}} \tag{2.12}$$

The spatial factor will be responsible for the convergence of quasi-static type, or more clearly, responsible for the exponential decrease of the envelope function (if such function existed). The temporal factor will affect spectral oscillations inside the envelope.

The results with the mode displacement method are given in figures 6 and 6. The results are quite the same between two truncated modes and eight truncated modes, even if the computation time is slightly larger for eight truncated terms. The M-norm shows also the same result.

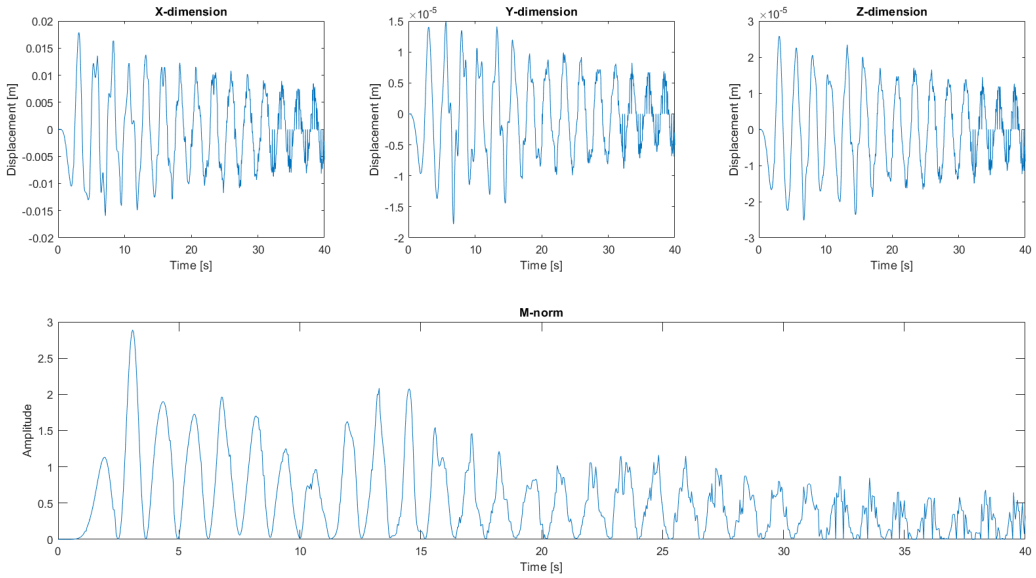


Figure 6: Mode displacement method, truncated to two modes
Computation time of .57s, time step of .04s

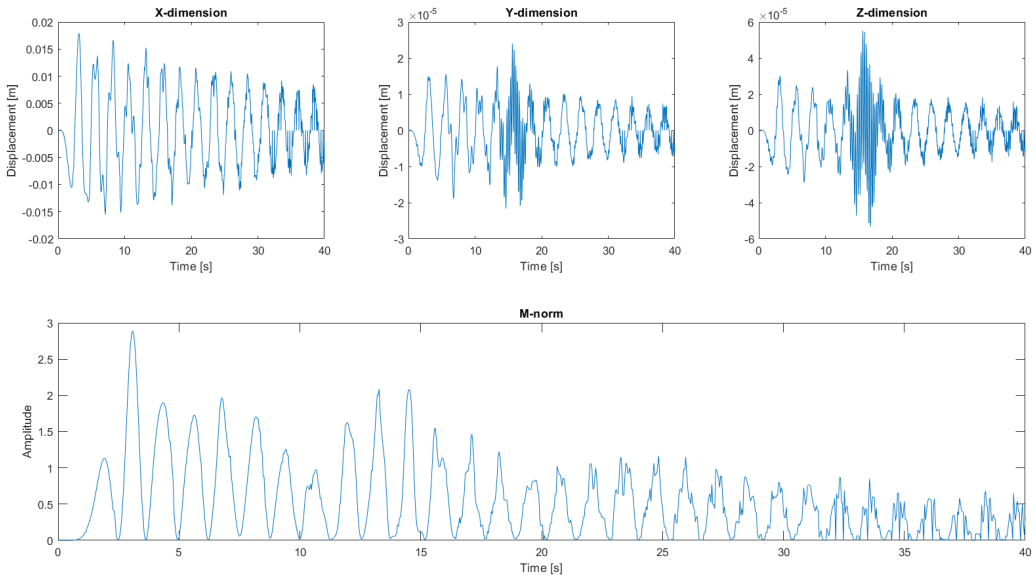


Figure 7: Mode displacement method, truncated to eight modes
Computation time of 2.11s, $h = .04$s

## 2.2 Mode acceleration method

This method takes into account the inertia and viscous forces in the truncated modal basis, which gives the following result

$$\boldsymbol{q}(t) = \boldsymbol{K}^{-1}\left[\boldsymbol{p}(t) - \sum_{r=1}^{k} \ddot{\eta}_r(t)\boldsymbol{M}\boldsymbol{x}_r - \sum_{r=1}^{k} \dot{\eta}_r(t)\boldsymbol{C}\boldsymbol{x}_r\right] \tag{2.13}$$

Rearranging the terms and taking advantage of the normal equations, the response vector is computed by the expression

$$\boldsymbol{q}(t) = \sum_{r=1}^{k} \eta_r(t)\boldsymbol{x}_r + \left(\boldsymbol{K}^{-1}\boldsymbol{p}(t) - \sum_{r=1}^{k} \frac{\phi_r(t)}{\omega_r^2}\boldsymbol{x}_r\right) \tag{2.14}$$

The expression recalls the one from the mode displacement method given in (2.10), with a corrective term

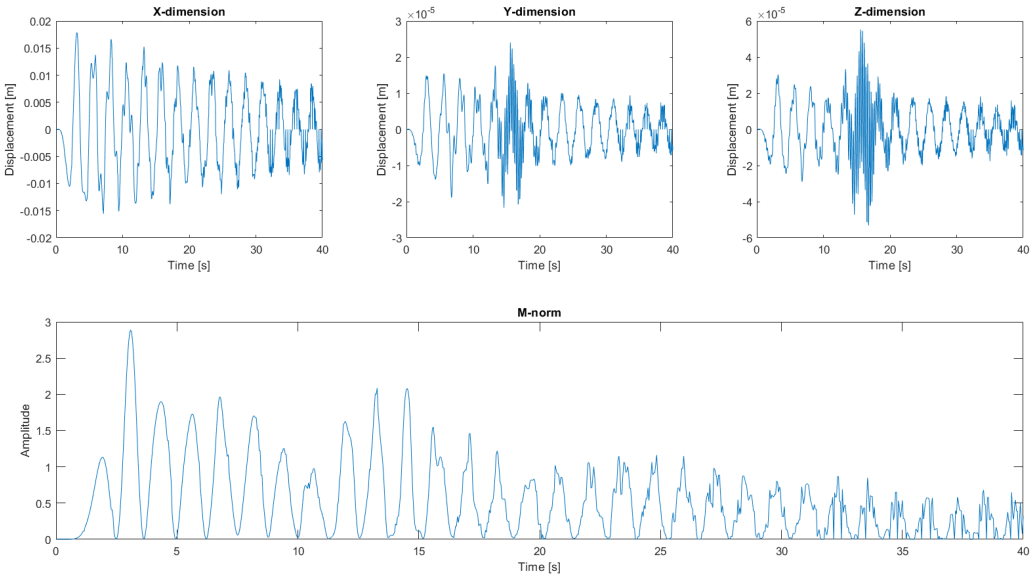


Figure 8: Mode acceleration method, truncated to eight modes
Computation time of 16.83s, $h = .04$s

## 2.3 Direct time integration - Newmark scheme

This method is stronger but much expensive in computation time. It doesn't take into account mode shapes calculated by the eigensystem, nor truncated serie. This method is based on direct numerical integration, thanks to the equation of motion and the initial conditions.

This method depends on a set of free parameters :

$$h; \quad \beta; \quad \gamma$$

. The first is the time step, paramount parameter in the standard numerical integration scheme, responsible for the accuracy of the evaluation of the derivative. The last ones are weight for the Taylor series expansions of the displacement and velocities, used in the evaluation of the integrals needed to calculate $\dot{\boldsymbol{q}}_{n+1}$ and $\boldsymbol{q}_{n+1}$. The values of theses parameters will affect convergence, numerical damping and stability of the scheme. The analysis of the residues yields that the values

$$\gamma = .5 \qquad \beta = 1/6$$

should minimize the error. But such parameters are subject to a stability limit, given by $\omega h \leq 3.46$. Figure 11 shows the instability of the integration scheme with such parameters.

The best choice in this case, for a structure with low natural frequencies, is a scheme unconditionally stable and without numerical damping. Such scheme is achieved with values

$$\gamma = .5 \qquad \beta = .25$$

and is called the *average constant acceleration* scheme. Nonetheless, this scheme yields a periodicity error of $\omega^2 h^2/12$, which can be minimised with a low time step, taking into account the low natural angular frequencies of the structure.

The flowchart of the computation of the method is presented in figure 9

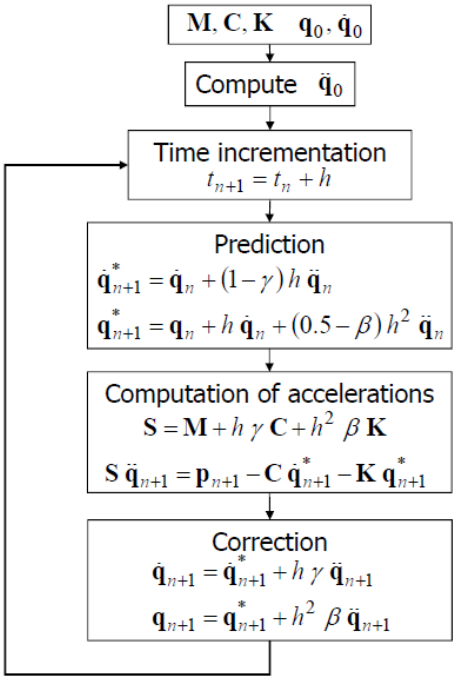


Figure 9: Newmark integration scheme flowchart [1]

As before, the initial conditions are set null :

$$\boldsymbol{q}(0) = \mathbf{0} \qquad \dot{\boldsymbol{q}}(0) = \mathbf{0} \longrightarrow \ddot{\boldsymbol{q}}(0) = \frac{\boldsymbol{p}(0)}{\boldsymbol{M}} \tag{2.15}$$

The results show the same displacements at the accelerometer degrees of freedom than the mode displacement and acceleration methods, but the M-norm of the displacement vector now yields a beautiful oscillating convergence exponentially decreasing, as stated by (2.12) :

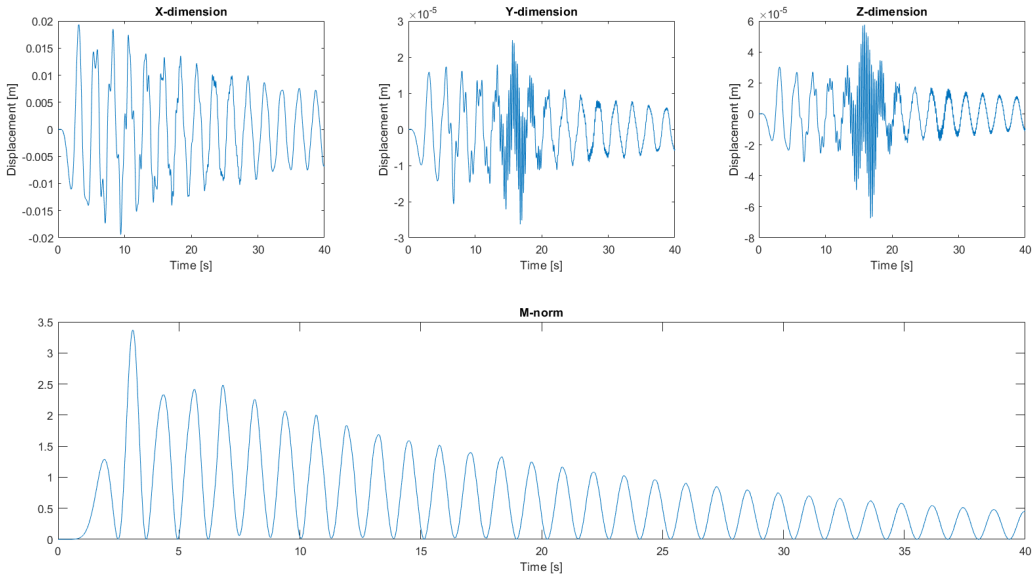


Figure 10: Newmark direct time integration scheme
Computation time of 54.17s, $h = .001$s, $\gamma = .5, \beta = .25$

The result with the same time step $h = .001$s and with parameters $\gamma = .5, \beta = 1/6$ (normally minimising error) shows indeed an unstable behaviour, reaching displacements of $10^{291}$ m :

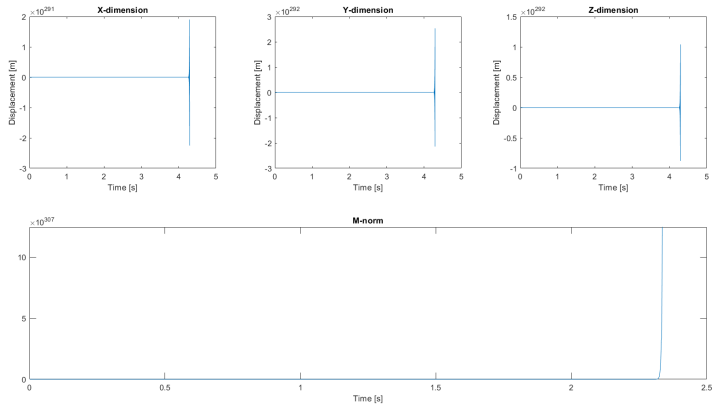


Figure 11: Newmark direct time integration scheme
Computation time of 73.46s, $h = .001$s, $\gamma = .5, \beta = 1/6$

The convergence of the Newmark integration scheme according to the time step is directly reached for $h = 10^{-2}$s. The evaluation of the frequency of the peak was made thanks to a discrete Fourier transform of the response vector calculated through the direct integration scheme.

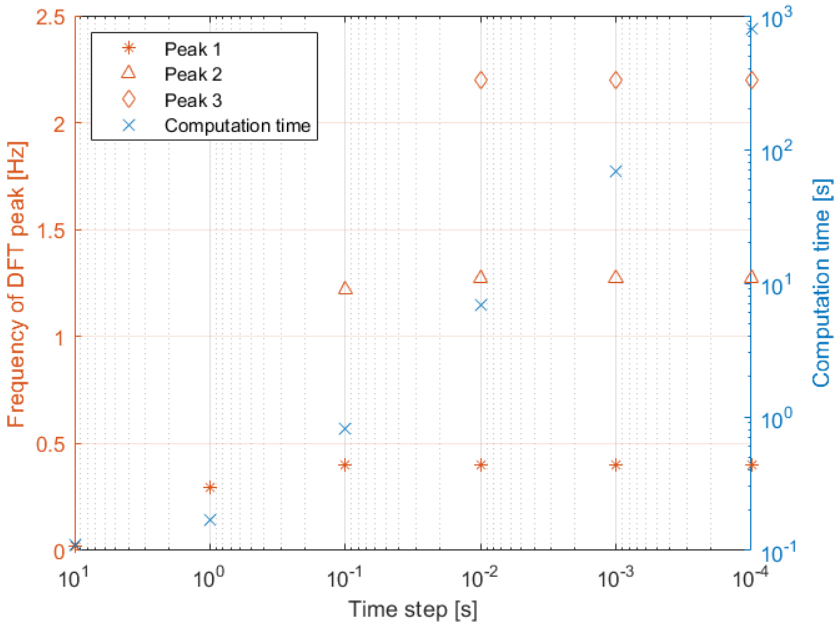


Figure 12: Convergence of the Newmark integration scheme according to time step for the three first peaks

According to the growing time step, less peaks could be distinguished, leading to less points of evaluation.

## 2.4 Methods comparison

### 2.4.1 Mode superposition methods

The difference between the two mode superposition methods is quite small, the maximal amplitude of the absolute difference of displacement hardly reaching $1\%$ of the calculated displacement. The average relative error calculated for each time step for a given number of truncated modes drops to less than $1\%$ as soon as the number of modes reaches $10$.

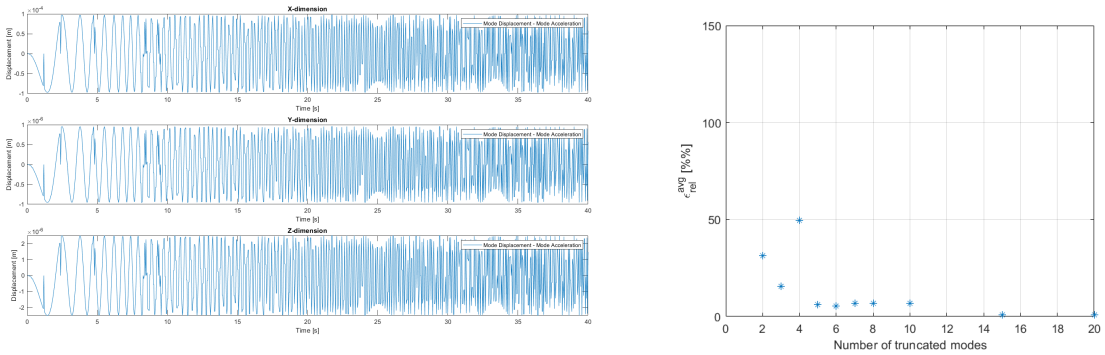


(a) Three dimensional absolute difference (b) Relative error

Figure 13: Comparison between mode superposition methods

This allows to conclude that the results of the mode superposition methods are almost the same.

However, the biggest difference resides in the computation time, as the mode acceleration method takes approximately ten times longer to compute.

### 2.4.2 Mode superposition and direct time integration methods

In this case, the difference is quite bigger. The absolute difference in displacement has an amplitude comparable to the displacement, in any direction. The average relative error is stagnating around $130\%$.

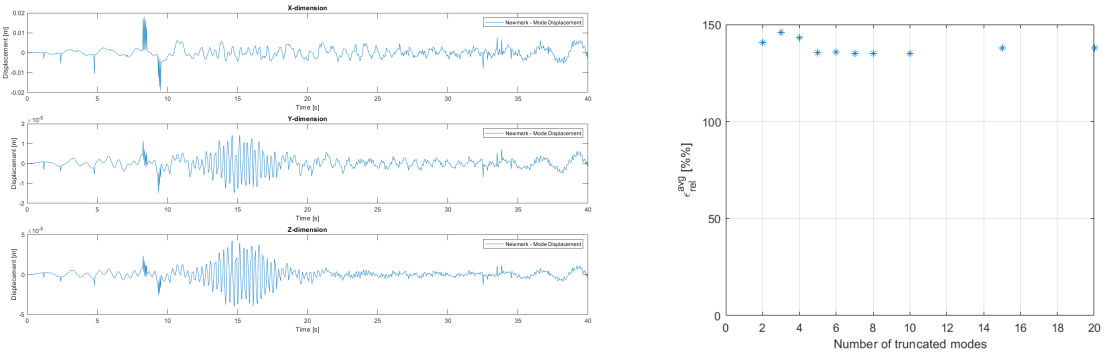


(a) Three dimensional absolute difference (b) Relative error

Figure 14: Comparison between direct time integration and mode superposition methods

However, the time of computation of the Newmark integration scheme is comparable to the mode displacement method, which both are ten times quicker to compute than the mode acceleration methods. This is a surprising result, as direct integration should be longer to compute than an approximation by a serie expansion in a subspace of the eigenmodes basis.

The Newmark scheme being known as a stronger method, taking into account directly the structural matrices and the initial conditions instead of the mode shapes extracted from the eigenvalue problem, this method should be preferred.

A discrete Fourier transform of the response vector shows

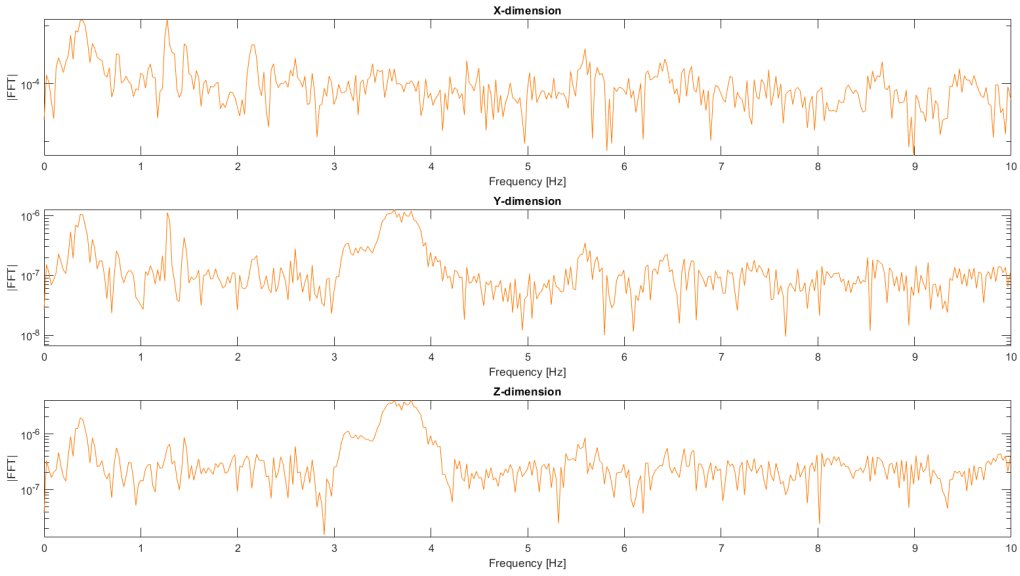


Figure 15: Discrete Fourier transform of the difference vector between Newmark and mode displacement methods

Where the peaks of highest amplitude correspond to the natural frequencies of the structure. Furthermore, a large peak is present in Y and Z directions and not in X direction, which could be explained by the fact that this eigenmode didn't yield a large deformation in the X dimension, giving then a similar result between the mode superposition and direct integration methods.

# 3 Model reduction

The reduction methods consist in a selection of a small amount of degrees of freedom compared to the total number, and to perform analysis on them. This yields a drastic diminution of the problem size, and then of the computation time, at the expense of a loss in calculus accuracy.

The reduction of the initial problem size $n$ to $k$ is made through the reduction matrix $\boldsymbol{R}$ of size $n \times k$

$$\boldsymbol{x} = \boldsymbol{R}\tilde{\boldsymbol{x}} \tag{3.1}$$

Where $\boldsymbol{x}$ is the initial mode shape of size $n \times 1$ and $\tilde{\boldsymbol{x}}$ is the reduced mode shape of size $k \times 1$. The structural matrices then transform as

$$\tilde{\boldsymbol{K}} = \boldsymbol{R}^T\boldsymbol{K}\boldsymbol{R} \qquad \tilde{\boldsymbol{M}} = \boldsymbol{R}^T\boldsymbol{M}\boldsymbol{R} \qquad \tilde{\boldsymbol{C}} = \boldsymbol{R}^T\boldsymbol{C}\boldsymbol{R} \tag{3.2}$$

Each of those square matrices are then of size $6 \times \#(\text{nodes retained})$ (here, four), where $6$ stands for the number of degree of freedom per node. This transforms the initial $n \times n$ eigenvalue problem stated in (1.6) to the reduced one of size $k \times k$

$$\tilde{\boldsymbol{K}}\tilde{\boldsymbol{x}} = \tilde{\omega}^2\tilde{\boldsymbol{M}}\tilde{\boldsymbol{x}} \tag{3.3}$$

In this work, the four nodes retained are shown in blue in the figure 16. To expand the study, other nodes have been considered : the red and the greens. They were considered only blue ones, or blue and red ones, or blue, red and green ones. This allow to study the behaviour and convergence of model reduction method according to the number of degrees of freedom retained, from $24$ to $72$.

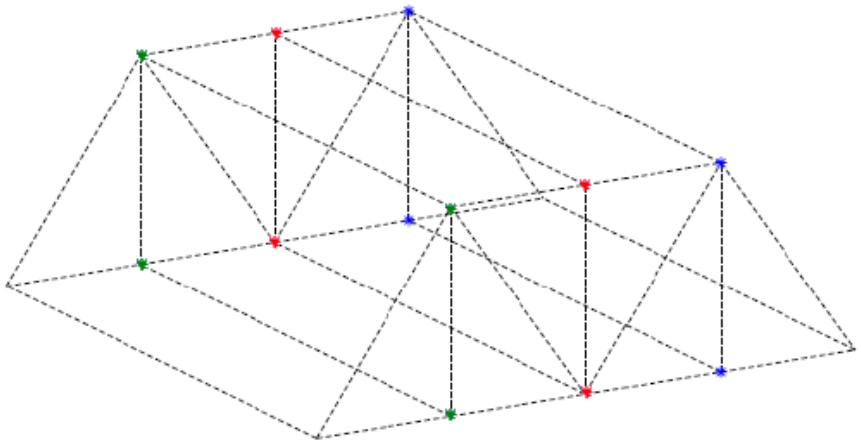

Figure 16: Nodes retained for the model reduction

Each structural matrix is subdivided into matrices corresponding to the size reduction chosen. Noting $C$ for the condensed nodes, and $R$ for the retained, the matrices are rewritten :

$$\boldsymbol{x} = \begin{bmatrix} \boldsymbol{x}_R \\ \boldsymbol{x}_C \end{bmatrix} \quad \boldsymbol{M} = \begin{bmatrix} \boldsymbol{M}_{RR} & \boldsymbol{M}_{RC} \\ \boldsymbol{M}_{CR} & \boldsymbol{M}_{CC} \end{bmatrix} \quad \boldsymbol{C} = \begin{bmatrix} \boldsymbol{C}_{RR} & \boldsymbol{C}_{RC} \\ \boldsymbol{C}_{CR} & \boldsymbol{C}_{CC} \end{bmatrix} \quad \boldsymbol{K} = \begin{bmatrix} \boldsymbol{K}_{RR} & \boldsymbol{K}_{RC} \\ \boldsymbol{K}_{CR} & \boldsymbol{K}_{CC} \end{bmatrix} \tag{3.4}$$

## 3.1 Guyan-Irons' reduction

### 3.1.1 Principle

The Guyan Irons' reduction method consists in a static condensation of the degrees of freedom, with the assumption that inertia forces may be neglected. This is equivalent to

$$\begin{bmatrix} \boldsymbol{K}_{RR} & \boldsymbol{K}_{RC} \\ \boldsymbol{K}_{CR} & \boldsymbol{K}_{CC} \end{bmatrix} \begin{bmatrix} \boldsymbol{x}_R \\ \boldsymbol{x_C} \end{bmatrix} = \begin{bmatrix} \boldsymbol{F}_R \\ \boldsymbol{F}_C \end{bmatrix} \text{ with } \boldsymbol{F}_C \approx 0 \tag{3.5}$$

This assumption $\boldsymbol{F}_C \approx 0$ corresponds to approximating that the mass corresponding to the condensed coordinates are neglected. This assumption directly gives an expression for the condensed part of the mode shape

$$\boldsymbol{x}_C = -\boldsymbol{K}_{CC}^{-1}\boldsymbol{K}_{CR}\boldsymbol{x}_R \tag{3.6}$$

Which helps to directly define the reduction matrix as

$$\boldsymbol{x} = \begin{bmatrix} \boldsymbol{x}_R \\ -\boldsymbol{K}_{CC}^{-1}\boldsymbol{K}_{CR}\boldsymbol{x}_R \end{bmatrix} = \begin{bmatrix} \mathbb{1} \\ -\boldsymbol{K}_{CC}^{-1}\boldsymbol{K}_{CR} \end{bmatrix} \boldsymbol{x}_R = \boldsymbol{R}\boldsymbol{x}_R \tag{3.7}$$

The method is said static because the reduction matrix is determined thanks to a static problem. Solving the eigenvalue problem stated in (3.2) with the reduced matrix of (3.2) then allows to estimate the natural frequencies.

### 3.1.2 Validity

A verification that the Guyan Irons' assumption is fulfilled and then that the method is valid is to evaluate and compare $\boldsymbol{F}_R$ and $\boldsymbol{F}_C$. From (3.5) we have

$$\begin{aligned} \boldsymbol{F}_R &= \boldsymbol{K}_{RR}\boldsymbol{x}_R + \boldsymbol{K}_{RC}\boldsymbol{x}_C \\ \boldsymbol{F}_C &= \boldsymbol{K}_{CR}\boldsymbol{x}_R + \boldsymbol{K}_{CC}\boldsymbol{x}_C \end{aligned} \tag{3.8}$$

The comparison of $\boldsymbol{F}_R$ over $\boldsymbol{F}_C$ will allow to estimate for the accuracy of the assumption and if the Guyan Irons method is relevant here. On the one hand, $\boldsymbol{F}_C$ needs to stay negligible, and above all negligible compared to $\boldsymbol{F}_R$. To estimate for the "smallness" of $\boldsymbol{F}_C$, its maximal value is

calculated. The ratio $\boldsymbol{F}_R/\boldsymbol{F}_C$ is then calculated by taking the minimal value of $\boldsymbol{F}_R$ divided by the maximal value of $\boldsymbol{F}_C$, and this through the modes calculated.

Across growing number of elements, a peculiar behaviour could not be detected. The calculations for $1, 2, 3, 5, 10$ and $20$ modes are averaged to give the final results, presented in the table 3.1. The values are quite stable, even if both decrease for a growing number of degrees of freedom retained. Nonetheless, the ratio goes hardly below $10{-}8$ while the maximal value of $\boldsymbol{F}_C$ hardly reaches $10^{-7}$, allowing to validate the Guyan Irons' method.

| DOFs | 24 | 48 | 72 |
|---|---|---|---|
| $\min\left(\boldsymbol{F}_R/\boldsymbol{F}_C\right)$ | $6.81\ 10^{9}$ | $2.97\ 10^{9}$ | $1.48\ 10^{9}$ |
| $\max\left(\boldsymbol{F}_C\right)$ | $1.62\ 10^{-7}$ | $8.30\ 10^{-8}$ | $7.41\ 10^{-8}$ |

Table 3.1: Evaluation of Guyan Irons' assumption average validity

### 3.1.3 Results

The relative error on the natural frequencies of the structure as computed by the Guyan-Irons' method has been computed for the eight first eigenmodes. The results are given in figure **??** and show that taking into account more degrees of freedom gives a better approximation of the frequencies, although the best accuracy on the first natural frequency is $0.37\%$.

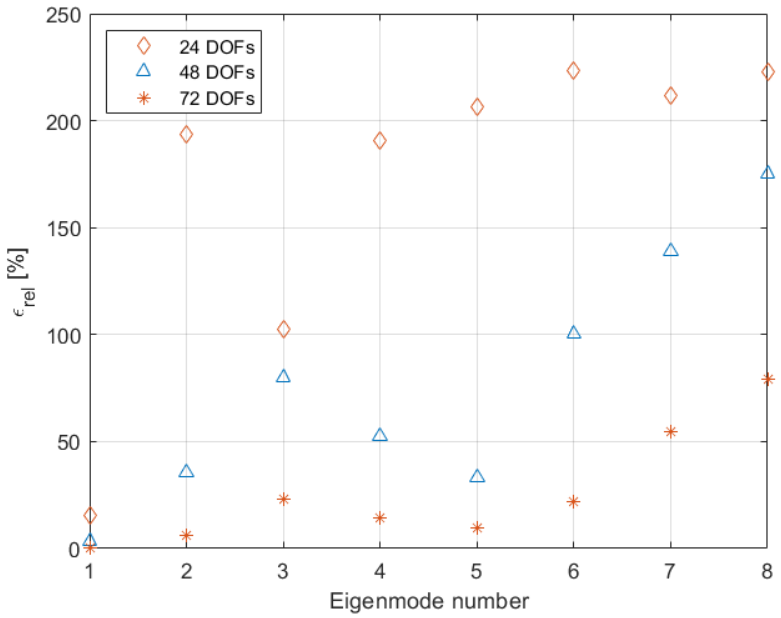


Figure 17: Relative error on the eigenfrequencies by the Guyan-Irons' method, for different number of degrees of freedom retained. Computed for a discretisation in 5 elements
Data available in table 3.2

| | 1 | 2 | 3 | 4 | 5 | 6 | 7 | 8 |
|---|---|---|---|---|---|---|---|---|
| 24 | 15.33% | 193.49% | 102.57% | 190.79% | 206.68% | 223.62% | 211.67% | 222.71% |
| 48 | 3.22% | 35.36% | 80.14% | 52.28% | 33.37% | 100.28% | 138.66% | 174.85% |
| 72 | .37% | 6.20% | 23.29% | 14.19% | 9.89% | 21.99% | 54.75% | 78.97% |

Table 3.2: $\varepsilon_{rel}$ on the peak frequencies for the Guyan-Irons' method according to the mode

## 3.2 Craig-Bampton's reduction

### 3.2.1 Principle

In contrast to the Guyan Irons' method, the Craig-Bampton's method is said dynamic, as it incorporates a new part containing eigenmodes clamped at their boundary. This comes from the fact that the dynamic behaviour of a substructure is fully described by [1] :

- The static modes resulting from imposed unit displacements on the boundary degrees of freedom
- The internal vibration modes of the subsystem clamped on the boundary

The reduction matrix then looks as follows

$$\boldsymbol{R}_{CB} = \begin{bmatrix} \mathbb{1} & 0 \\ -\boldsymbol{K}_{CC}^{-1}\boldsymbol{K}_{CR} & \boldsymbol{X} \end{bmatrix} \tag{3.9}$$

Where $\boldsymbol{X}$ represents the fixed interface modes. In practice, the internal modes are truncated.

### 3.2.2 Results and convergence

The relative error averaged on the eight first eigenmodes has been computed according to the number of modes taken into account in the Craig-Bampton's method. The results are presented in figure 18, which exceptionally presents continuous lines to get a more clear view of the behaviour. As one can see, more degrees of freedom allows for a better approximation when few modes are taken into account (for one mode we have $120.35\%$ for $24$ DOFs and $14.93\%$ for $72$ DOFs). Nonetheless, when the number of modes reaches high values, it seems more precise to use a low number of degrees of freedom.

The computation time seems proportionally linear with the number of modes.

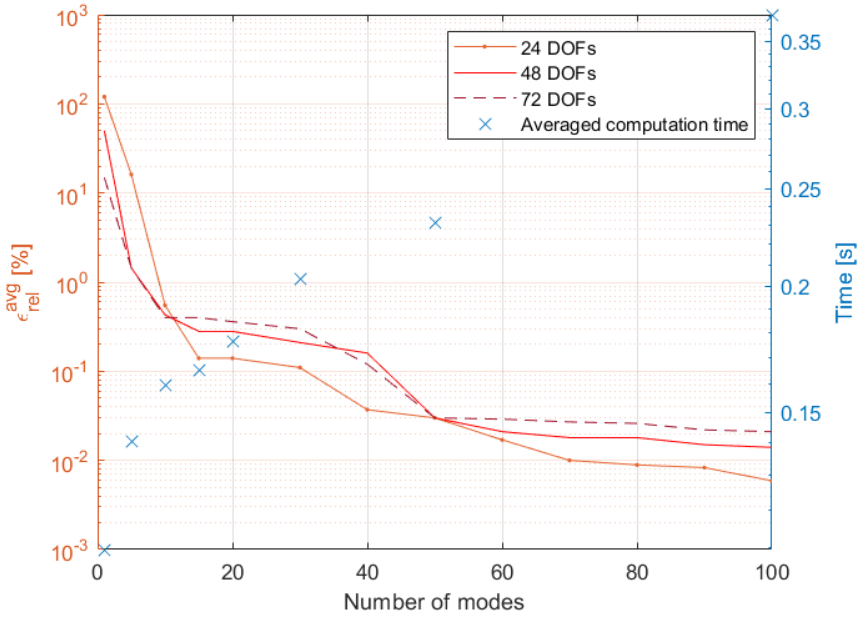


Figure 18: Comparison of relative error on the peak frequency averaged on the eight first eigenmodes and time of computation for different number of modes in Craig-Bampton's method, for 24 degrees of freedom retained, computed for a discretisation in 5 elements

Obviously, the Craig-Bampton's method seems the best choice to make in this case. Nonetheless, the increasing computation time has to be taken into account, mainly for very great number of degrees of freedom. In this case, the Guyan-Irons is a good alternative for a fast and quite good approximation of the natural frequencies.

# 4 Conclusion

This work aimed at modelling a simple structure and perform a dynamic analysis on it, by the means of the *FEM - Finite Element Method* which consists of discretising the structure in sub-elements. An existing solver, SAMCEF from 9Siemens NX and a program created using MATLAB and based on methods seen in the *Theory of Vibration* course taught at Université de Liège [1] were used. The first one accounts for the exact solutions, to compare for accuracy of the handmade program.

Both calculated same natural frequencies up to a limit on the accuracy of the MATLAB model. A study on the convergence of the frequencies calculated according to the discretisation was performed, showing a very fast convergence (observed as soon as $N_{el} \geq 5$) asymptotic to $\varepsilon_{rel} \approx 1\%$ of the MATLAB model. This is explained by the differences in parameters taken into account for the computation between the two solvers (the shear stress e.g. is taken into account in SIEMENS NX). The computation of stiffness and mass matrices allowed to draw the first mode shapes corresponding to the natural frequencies, and to analyse the deformations occurring.

The next step was to simulate the action on a node of a one dimensional shaker whose time dependant signal is a chirped sine wave (going from null frequency to $10$ Hz in $40$s). The shaker acted in the $X$ dimension of the bridge. To account for results, the displacement in response to this external excitation was simulated as if a three dimensional accelerometer was recording at another node. Two families of methods were computed. The first one is *modal superposition*, with mode displacement and mode acceleration methods. The impact of the number of terms, the time step and the computation time were compared. The second one is *direct time integration*, followed with the Newmark scheme. An analysis of the impact of the free parameters of this method, weights $\gamma$, $\beta$ and the time step $h$, has been performed. The values pf $\gamma = .5$ and $\beta = .25$ have been chosen, following the constant acceleration scheme, to ensure unconditional stability and no numerical damping.

Modal superposition methods show very similar results, with an averaged relative error dropping to $1\%$ as soon as $10$ sub elements were computed. Between direct time integration and modal superposition, the difference was not negligible, as the amplitude was comparable to displacement amplitude. The difference between the methods mainly peaked at natural frequencies of the structure. This is explained by the fact that modal superposition methods are based on a truncated subspace of the eigenmode basis, while the Newmark integration scheme computes directly from the structural matrices. Nonetheless, each method shows consistent results, in amplitude and displacement shape.

Finally, the structure is condensed using Guyan-Irons' static and Craig Bampton's dynamic methods. Model reduction is used because of too large number of degrees of freedom or number of elements, and allows for a estimation of the natural frequencies with great decrease of the computation time, at the expense of precision. The Guyan Irons' method is based on an assumption which is verified to validate the use of the method in this case. It yields results with an averaged relative error of roughly $170\%$ with twenty-four degrees of freedom retained, around $75\%$ for forty-eight degrees of freedom, and approximately $25\%$ for seventy-two. The average has been computed on the eight first eigenmodes, for the first natural frequency we have $\varepsilon_{rel} = 15.33\%$ for twenty-four, $\varepsilon_{rel} = 3.22\%$ for forty-eight and $\varepsilon_{rel} = 0.37\%$ for seventy-two.

# References

[1] J.-C. Golinval. *Theory of Vibration - MECA-0029*. School of Engineering - Université of Liège, 2019 (cit. on pp. 14, 22, 24).

[2] M. Géradin and D. J. Rixen. *Mechanical Vibrations : Theory and Application to Structural Dynamics*. 3rd ed. John Wiley & Sons, Ltd, 2015. ISBN: 978-1-118-90020-8.